PHYSICAL REVIEW C **87**, 034309 (2013)

Evolution of single-particle states beyond ^{132}Sn

L. Coraggio,[1] A. Covello,[1,2] A. Gargano,[1] and N. Itaco[1,2]

[1]*Istituto Nazionale di Fisica Nucleare, Complesso Universitario di Monte S. Angelo, I-80126 Napoli, Italy*

[2]*Dipartimento di Fisica, Università di Napoli Federico II, Complesso Universitario di Monte S. Angelo, I-80126 Napoli, Italy*

(Received 15 January 2013; published 7 March 2013)

We have performed shell-model calculations for the two one-valence-neutron isotones ^{135}Te and ^{137}Xe and the two one-valence-proton isotopes ^{135,137}Sb. The main aim of our study has been to investigate the evolution of single-particle states with increasing nucleon number. To this end, we have focused attention on the spectroscopic factors and the effective single-particle energies. In our calculations, we have employed a realistic low-momentum two-body effective interaction derived from the CD-Bonn nucleon-nucleon potential that has already proved quite successful in describing the spectroscopic properties of nuclei in the ^{132}Sn region. Comparison shows that our results reproduce very well the available experimental data. This gives confidence in the evolution of the single-particle states predicted by the present study.

DOI: 10.1103/PhysRevC.87.034309 PACS number(s): 21.60.Cs, 21.30.Fe, 21.10.Jx, 27.60.+j

I. INTRODUCTION

The evolution of single-particle states when moving away from double shell closures has long been a subject of primary interest in nuclear structure physics. It was in the early 1960s [1], in fact, that quantitative experimental information on this subject started to become available thanks to the study of one-nucleon transfer reactions such as (d,p) and (d,t). During the 1960s and early 1970s, the field developed rapidly and spectroscopic factors were extracted from pickup and stripping reactions for many nuclei. In particular, the stable Sn isotopes and $N = 82$ isotones were the subject of extensive studies [2,3] which provided relevant information on the shell-model structure of these nuclei. By the end of the 1970s, however, most of the feasible experiments had been performed and the study of transfer reactions began loosing its role as a most powerful tool for the understanding of nuclear structure.

As it was to be expected, the advent of radioactive ion beams (RIBs) has opened a new era for the study of transfer reactions, which is currently recognized as one of the major research themes to be pursued at the second-generation RIB facilities. A main feature of transfer reactions with RIBs is that they have to be performed in inverse kinematics. This is for instance the case of the ^{132}Sn(d,p) reaction recently performed at the first-generation RIB facility at Oak Ridge National Laboratory [4,5]. This experiment allowed the investigation of the single-particle structure of the one-valence-neutron nucleus ^{133}Sn; the spectroscopic factors for the ground and three excited states extracted from the differential cross sections turned out to be very close to one. This is a remarkable achievement which has set the stage for future studies of neutron-rich nuclei in the ^{132}Sn region, which are also of great interest for modeling *r* process nucleosynthesis.

In this context, it is worth mentioning that it is also of current interest the study of transfer reactions with stable beams in inverse kinematics to test new detectors specifically designed for use with heavy beams. A recent notable example of this kind of study is the ^{136}Xe (d,p) reaction performed at the ATLAS facility at Argonne National Laboratory [6], which has provided a stringent test of the HELIOS spectrometer used to analyze the outgoing protons.

Experimental studies of nucleon transfer reactions currently going on and the bright perspectives for future research with RIBs are of course a great stimulus for theoretical studies aimed at understanding the evolution of single-particle states. This is indeed the case of our very recent shell-model study [7] of the single-neutron properties of ^{137}Xe, which received motivation from the experiment of Ref. [6].

Based on the results obtained in [7], we have found it very interesting to perform a similar study for other nuclei beyond ^{132}Sn which are within reach of (d,p) transfer reactions with RIBs. More precisely, we consider the two one-valence-neutron isotones ^{135}Te and ^{137}Xe and the two one-valence-proton isotopes ^{135,137}Sb. Actually, results for ^{137}Xe have already been given in [7], where we essentially focused on the comparison between our spectroscopic factors and those reported in [6]. The present paper is of more general scope, in that we study how the single-particle states of ^{133}Sb and ^{133}Sn are modified by the addition of pairs of neutron and protons, respectively.

The article is organized as follows. In Sec. II we give an outline of our calculations. In Sec. III the results for the energies and spectroscopic factors are presented and discussed in detail. In Sec. IV we present our predicted effective single-particle energies and discuss their evolution. Section V contains a summary of our conclusions.

II. OUTLINE OF CALCULATIONS

The results presented in this section have been obtained with the same Hamiltonian used in our previous shell-model studies of neutron-rich nuclei beyond ^{132}Sn [8–10]. In this Hamiltonian, the single-particle energies are taken from experiment while the two-body effective interaction is derived within the framework of perturbation theory [11,12] starting from the CD-Bonn NN potential [13] renormalized by way of the $V_{\mathrm{low-k}}$ approach [14]. Some details on the calculation of this two-body interaction can be found in [7]. We discuss here only the choice of the single-particle energies that may be relevant to the discussion of our results.

We assume that the valence protons and neutrons occupy the first major shells outside doubly magic ^{132}Sn. Namely,

TABLE I. Single-proton and -neutron energies (in MeV).

$\pi(n,l,j)$	ϵ	$\nu(n,l,j)$	ϵ
$0g_{7/2}$	0.000	$1f_{7/2}$	0.000
$1d_{5/2}$	0.962	$2p_{3/2}$	0.854
$2d_{3/2}$	2.439	$2p_{1/2}$	1.363
$0h_{11/2}$	2.793	$0h_{9/2}$	1.561
$2s_{1/2}$	2.800	$1f_{5/2}$	2.005
		$0i_{13/2}$	2.694

protons are allowed to move in the five orbits $0g_{7/2}$, $1d_{5/2}$, $1d_{3/2}$, $0h_{11/2}$, and $2s_{1/2}$ of the 50–82 shell and neutrons in the six orbits $1f_{7/2}$, $2p_{3/2}$, $0h_{9/2}$, $2p_{1/2}$, $1f_{5/2}$, and $0i_{13/2}$ of the 82–126 shell.

The adopted single-proton and -neutron energies are shown in Table I. For protons, the first four are taken to be the experimental energies of the levels with corresponding spin and parity in ^{133}Sb [15]. The energy of the $s_{1/2}$ orbit, which is still missing, is taken from [16], where it was determined by reproducing the experimental energy of the $1/2^+$ state at 2.150 MeV in ^{137}Cs. This is, in fact, populated with significant strength in the ^{136}Xe(^{3}He, d)^{137}Cs transfer reaction [3], while no $1/2^+$ state has been yet identified in the lighter $N = 82$ isotone, ^{135}I. It is worth noting that no spectroscopic factors are available for the states of ^{133}Sb, which has been mainly studied by β-decay experiments in the 1990s [17].

As already mentioned in the Introduction, the single-neutron nature of the observed states in ^{133}Sn has been recently studied in a (d,p) transfer reaction with a ^{132}Sn RIB [4,5]. In this experiment, the spectroscopic factors of the previously observed [18] $7/2^-$, $3/2^-$, and $5/2^-$ states were extracted evidencing little fragmentation of the single-particle strength. Furthermore, a strong candidate for the $2p_{1/2}$ single-particle orbit was identified at 1.363 MeV excitation energy, which is about 300 keV lower than the previous proposed value [18]. A state at 1.561 MeV was not significantly populated in this (d,p) reaction. This state, associated with $J^\pi = 9/2^-$ in previous β decay [18] and spontaneous fission [19] experiments, is expected to correspond to the $0h_{9/2}$ orbit. The $13/2^+$ state has not yet been observed in ^{133}Sn and the energy reported in Table I has been estimated from that (2.434 MeV) of the experimental 10^+ state in ^{134}Sb, assumed to belong to the $\pi g_{7/2}\nu i_{13/2}$ configuration. The shell-model calculations have been performed by using the OXBASH code [20].

III. ENERGIES AND SPECTROSCOPIC FACTORS: RESULTS AND DISCUSSION

In this section, we present and discuss our results for ^{135}Te and ^{137}Xe with two and four protons in addition to ^{133}Sn, as well as those for ^{135}Sb and ^{137}Sb with two and four neutrons in addition to ^{133}Sb. We focus attention on the energies and spectroscopic factors of states with angular momentum and parity corresponding to those of the single-neutron and -proton orbits for $N = 83$ isotones and Sb isotopes, respectively. In fact, it is a main aim of our study to find out whether states with single-particle character survive when adding nucleon pairs and to which extent this depends on the nature of the added pairs.

TABLE II. Calculated energies and spectroscopic factors for states in ^{135}Te. The available experimental data are reported for comparison (see text for details).

Calc.			Expt.	
J^π	E(MeV)	C^2S	J^π	E(MeV)
$(1/2^-)_1$	1.110	0.45	$(1/2^-)$	1.083
$(1/2^-)_2$	1.947	0.32		
$(1/2^-)_3$	2.400	0.16		
$(3/2^-)_1$	0.726	0.63	$(3/2^-)$	0.659
$(3/2^-)_2$	1.721	0.27		
$(5/2^-)_1$	1.119	0.12	$(5/2^-)$	1.127
$(5/2^-)_6$	2.238	0.41		
$(7/2^-)_1$	0.000	0.88	$(7/2^-)$	0.000
$(9/2^-)_1$	1.302	0.18	$(9/2^-)$	1.246
$(9/2^-)_2$	1.346	0.51	$(7/2^-,9/2^-)$	1.380
$(9/2^-)_5$	2.214	0.07		
$(9/2^-)_6$	2.308	0.07		
$(13/2^+)_1$	2.268	0.72	$(13/2^+)$	2.109
$(13/2^+)_2$	3.356	0.19		

A. ^{135}Te and ^{137}Xe

Let us start with the $N = 83$ isotones. Excitation energies and spectroscopic factors for ^{135}Te and ^{137}Xe are shown in Tables II and III, respectively, where only states with $C^2S \geqslant 0.07$ are included. In Table III, we also show the energies and spectroscopic factors obtained in [6] for levels which can be safely identified with the calculated ones. For a detailed comparison between experiment and theory, we refer to [7] while here some points relevant to the present discussion will be considered. For ^{135}Te only experimental energies are available [15], although a (d,p) reaction on

TABLE III. Calculated energies and spectroscopic factors for states in ^{137}Xe. The available experimental data are reported for comparison (see text for details).

Calc.			Expt.		
J^π	E(MeV)	C^2S	J^π	E(MeV)	C^2S
$(1/2^-)_1$	1.127	0.43	$1/2^-,3/2^-$	0.986	0.35
$(1/2^-)_2$	1.926	0.13			
$(1/2^-)_4$	2.305	0.18			
$(1/2^-)_5$	2.407	0.07			
$(3/2^-)_1$	0.728	0.57	$3/2^-$	0.601	0.52
$(3/2^-)_2$	1.708	0.07			0
$(3/2^-)_3$	1.783	0.15			
$(5/2^-)_1$	1.349	0.17	$5/2^-$	1.303	0.22
$(5/2^-)_5$	2.039	0.20			
$(7/2^-)_1$	0.000	0.86	$7/2^-$	0.000	0.94
$(9/2^-)_1$	1.327	0.72	$9/2^-$	1.218	0.43
$(13/2^+)_1$	2.082	0.75	$(13/2^+)$	1.751	0.84

^{134}Te was performed at HRIBF [21]. In fact, preliminary tentative results from this experiment do not allow to extract spectroscopic factors but only to identify the $7/2^-$ ground state and the $1/2^-$ and $3/2^-$ yrast states as resulting from the $l = 3$ and 1 transfers, respectively. In this connection, it should be mentioned that the nuclei ^{135}Te and ^{137}Xe have been recently studied by (^{13}C, ^{12}Cγ) and (^{9}Be, ^{8}Beγ) direct reactions in inverse kinematics, leading to an high precision measurement of the excitation energy of the yrast $13/2^+$ state in both nuclei [22].

From Tables II and III we see that the agreement between experimental and calculated energies is very good. The largest discrepancy in both ^{135}Te and ^{137}Xe is found for the $13/2^+$ state, which is overestimated by 150 and 330 keV, respectively. In this connection, it is worth mentioning that its position is directly related to the energy of the $0i_{13/2}$ level, which, as mentioned in the previous section, is still missing.

Our calculations for ^{135}Te confirm the preliminary results of [21], the $7/2^-$, $1/2^-$, and $3/2^-$ yrast states having, in fact, the largest spectroscopic factors. Actually, it turns out that this $7/2^-$ state, as well as the yrast $13/2^+$ state, carries the largest fraction of the single-particle strength, while a non-negligible percentage of the $p_{1/2}$ and $p_{3/2}$ strengths is distributed over higher-energy states. As for the $J^\pi = 9/2^-$ states, we find that it is the yrare state at 1.346 MeV to have the largest spectroscopic factor, 0.51, to be compared to 0.18 for the yrast one. These predicted two $9/2^-$ states are quite close in energy, the difference being only a few tens of keV. Note that a state at 1.380 MeV has been observed with no firm spin assignment $(7/2^-, 9/2^-)$, which could be associated either with our second $9/2^-$ state or our second $7/2^-$ state at 1.336 MeV with $C^2S = 0.06$. Finally, we see that the largest strength of the $f_{5/2}$ orbit is predicted to be carried by the sixth $5/2^-$ state at 2.238 MeV, $C^2S = 0.41$, while the spectroscopic factors of the lowest five states are much smaller.

When one adds two more protons going from ^{135}Te to ^{137}Xe, a state of a single-particle nature can be still identified for each J^π, which is the yrast state, except for $J^\pi = 5/2^-$. As for the $f_{5/2}$ strength, a stronger fragmentation is found in ^{137}Xe with respect to ^{135}Te, the highest spectroscopic factor being 0.20 for the fifth excited state. Our findings for ^{137}Xe are consistent with the experimental results, although the spectroscopic factor of the yrast $9/2^-$ state is overestimated by the theory. This point is discussed in Ref. [7].

Based on the above considerations, we have found it interesting to compare the adopted single-neutron energies for ^{133}Sn with the calculated spectra of ^{135}Te and ^{137}Xe, including, for each J^π, only the level with the largest spectroscopic factor. This is done in Fig. 1, where we see that when adding proton pairs to ^{133}Sn the single-neutron spectrum preserves its original structure, becoming on the whole slightly more compressed. Actually, only the $5/2^-$ state in both nuclei moves up in energy. In this context, it may be worth mentioning that the lower $5/2^-$ states, which are not of a single-particle nature, are predicted by our calculations to arise from the coupling of the single-neutron $f_{7/2}$ state to two-proton excitations. The 2^+, 4^+, and 6^+ in ^{134}Te lie, in fact, at an energy ranging from 1.3 to 1.7 MeV, which is lower than that, 2.0 MeV, of the $f_{5/2}$ level in ^{133}Sn.

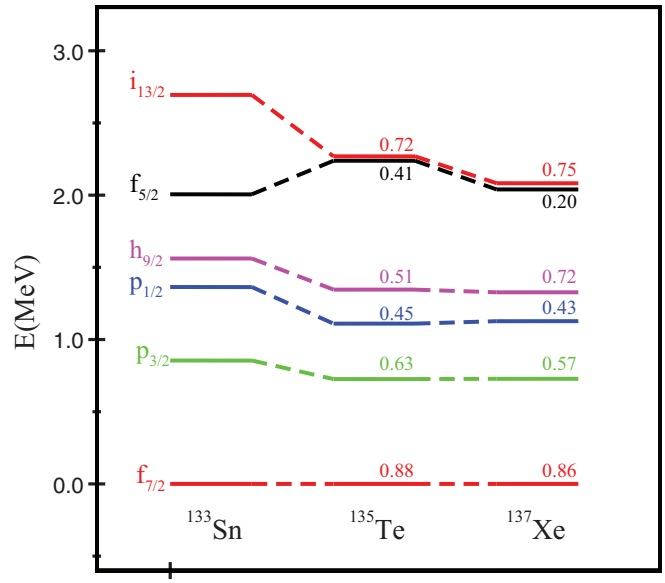

FIG. 1. (Color online) Calculated energy levels with corresponding spectroscopic factors in the $N = 83$ isotones ^{135}Te and ^{137}Xe (see text for details). Single-neutron levels for ^{133}Sn are also reported.

B. ^{135}Sb and ^{137}Sb

The energies and spectroscopic factors for ^{135}Sb and ^{137}Sb are reported in Tables IV and V, respectively, including only states with $C^2S \geqslant 0.07$ selected among the lowest twenty states for each angular momentum. For ^{137}Sb only the ground state is known, while for ^{135}Sb several states have been observed, most of them, however, without firm spin assignment. Furthermore, no spectroscopic factors have been obtained. In Table IV the experimental energies of ^{135}Sb [15]

TABLE IV. Calculated energies and spectroscopic factors for states in ^{135}Sb. The available experimental data are reported for comparison (see text for details).

Calc.			Expt.	
J^π	E(MeV)	C^2S	J^π	E(MeV)
$(1/2^+)_1$	0.659	0.07	$(1/2^+)$	0.523
$(1/2^+)_{11}$	2.880	0.07		
$(1/2^+)_{12}$	3.119	0.32		
$(1/2^+)_{15}$	3.476	0.17		
$(3/2^+)_1$	0.497	0.07	$(3/2^+)$	0.440
$(3/2^+)_3$	1.320	0.07		
$(3/2^+)_{12}$	2.600	0.32		
$(3/2^+)_{13}$	2.697	0.10		
$(3/2^+)_{14}$	2.768	0.09		
$(5/2^+)_1$	0.387	0.42	$(5/2^+)$	0.282
$(5/2^+)_2$	0.928	0.23		
$(5/2^+)_5$	1.657	0.09		
$(5/2^+)_8$	1.950	0.14		
$(7/2^+)_1$	0.000	0.74	$(7/2^+)$	0.000
$(7/2^+)_2$	0.944	0.18		
$(11/2^-)_1$	2.652	0.52		
$(11/2^-)_2$	3.132	0.11		
$(11/2^-)_5$	3.522	0.21		

TABLE V. Calculated energies and spectroscopic factors for states in ^{137}Sb.

	Calc.	
J^π	E(MeV)	C^2S
$(1/2^+)_1$	0.403	0.11
$(3/2^+)_1$	0.333	0.12
$(5/2^+)_1$	0.186	0.53
$(5/2^+)_{10}$	1.538	0.09
$(7/2^+)_1$	0.000	0.71
$(7/2^+)_2$	0.913	0.09
$(11/2^-)_1$	2.587	0.38
$(11/2^-)_2$	2.848	0.15

for states which can be safely associated with the calculated ones are shown and we see that they are very well reproduced by the theory.

As regards the spectroscopic factors, the calculated values for both nuclei evidence a strong fragmentation of the single-particle strength with respect to ^{135}Te and ^{137}Xe. We find, in fact, that in ^{135}Sb only for three J^π, which reduce to two in ^{137}Sb, there is one state with a spectroscopic factor larger than 0.4. The remaining strength in both nuclei is shared between

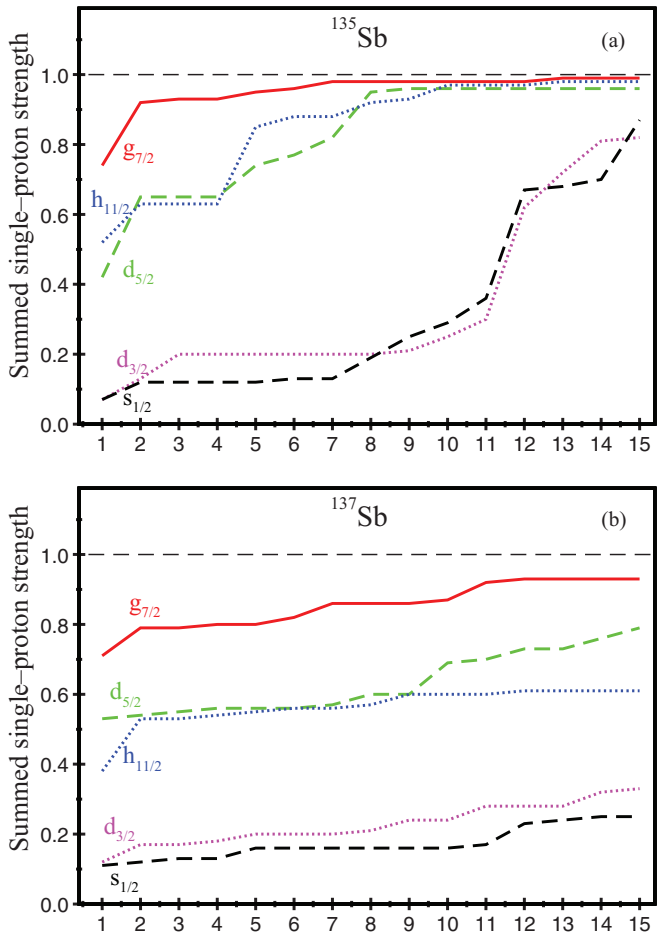

FIG. 2. (Color online) Summed spectroscopic factors for (a) ^{135}Sb and (b) ^{137}Sb as a function of the included states (see text for details).

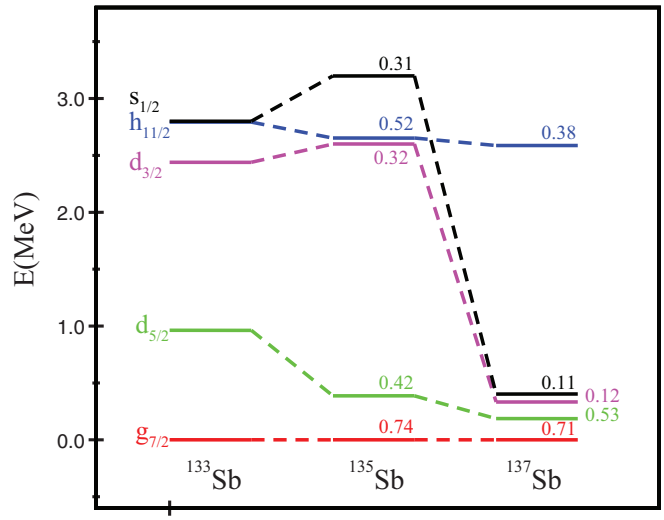

FIG. 3. (Color online) Calculated energy levels with corresponding spectroscopic factors in the $Z = 51$ isotopes ^{135}Sb and ^{137}Sb (see text for details). Single-proton levels for ^{133}Sb are also reported.

many states. We have seen in Sec. III A that for the $N = 83$ isotones this occurs only for $J^\pi = 5/2^-$ in ^{137}Xe.

The spreading of the single-proton strength in the $Z = 51$ isotopes can be better seen through the cumulative sum of the spectroscopic factors, which is shown in Fig. 2 for each single-proton orbit as a function of the number of states included in the sum. We see that the fragmentation is particularly strong for the $s_{1/2}$ and $d_{3/2}$ strengths, which in ^{137}Sb do not reach significant values even when including the 15 lowest-lying states.

As a direct consequence of the large fragmentation induced by addition of neutron pairs, the single-particle spectrum of ^{133}Sb is substantially modified, as shown in Fig. 3 which is the counterpart of Fig. 1. This occurs already in ^{135}Sb with only two more neutrons, the most noticeable change being the lowering of the $5/2^+$ state by about 600 keV.

The low position of the $5/2^+$ state in ^{135}Sb has been indeed in focus of great attention [23,24]. In some studies, this was traced to a decrease of the proton $d_{5/2}$-$g_{7/2}$ spacing produced by the two neutrons beyond the $N = 82$ shell closure. On the other hand, our predicted spectroscopic factor, 0.42, evidences that this state has no strong single-particle nature, namely non-negligible components with seniority larger than one are contained in its wave function. This was discussed in detail in Ref. [23], where we showed that the seniority-one state $|\pi d_{5/2}(\nu f_{7/2})^2_{J=0}\rangle$, with an unperturbed energy of 0.962 MeV, is pushed down by the neutron-proton interaction getting admixed with the seniority-three state $|\pi g_{7/2}(\nu f_{7/2})^2_{J=2}\rangle$, which lies at 0.368 MeV.

This mechanism explains indeed the fragmentation of the single-particle strength we predict for almost all states in both ^{135}Sb and ^{137}Sb. By the same token, we see why no strong fragmentation is found for the $N = 83$ isotones, most of the seniority-one states lying, in this case, sufficiently lower in energy with respect to the seniority-three states. This difference in the evolution of the single-proton versus

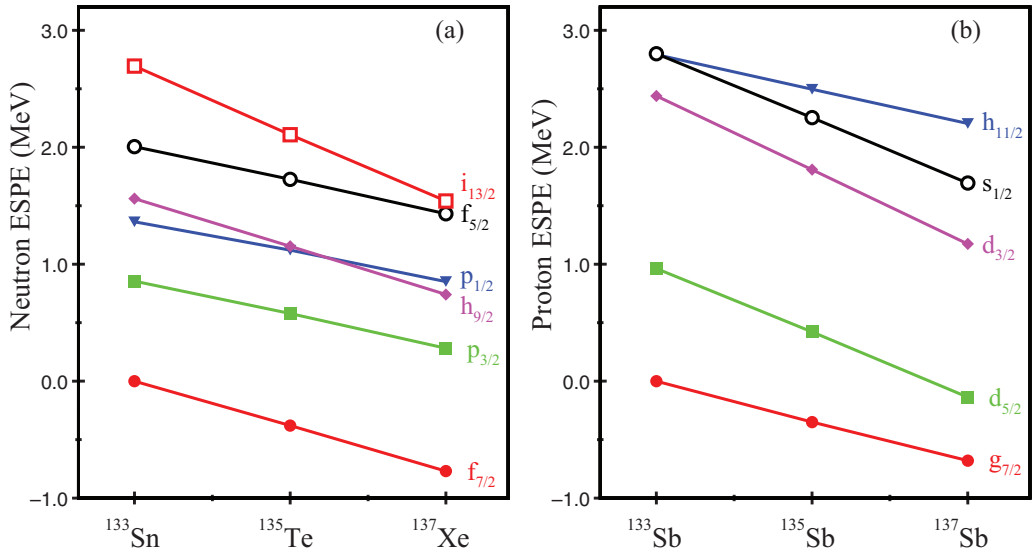

FIG. 4. (Color online) Evolution of (a) neutron and (b) proton ESPEs.

single-neutron states may be then traced to the different pairing force acting between protons and neutrons.

It is indeed a feature of our effective interaction to have different pairing properties for protons above $Z = 50$ and neutrons above $N = 82$, which results in a "normal" pairing for protons and a significantly weaker pairing for neutrons. In our derivation of the effective interaction, this arises from the second-order core polarization effects, the main role being played by one-particle–one-hole excitations [25]. Experimentally, the reduction of neutron pairing is clearly manifested by the large difference between the proton and neutron gap in ^{134}Te and ^{134}Sn, the latter being about 0.5 MeV smaller than the former.

IV. EFFECTIVE SINGLE-PARTICLE ENERGIES

In this section we discuss the single-proton and -neutron energies which can be associated to the underlying mean field when neutron and proton pairs are added to ^{133}Sb or ^{133}Sn, respectively. These quantities are the effective single-particle energies (ESPEs) [26,27]

$$\bar{\epsilon}_{j_\rho} = \epsilon_{j_\rho} + \sum_{j_{\rho'}} V^M(j_\rho j_{\rho'}) N_{j_{\rho'}}, \qquad (1)$$

where ρ and ρ' stand for neutron and proton index, respectively, or vice versa. For a given j_ρ, ϵ_{j_ρ} denotes the corresponding energy in the one-valence system and N_{j_ρ} the occupation number in the ground state of the even-even system, while

$$V^M(j_\rho j_{\rho'}) = \frac{\sum_J (2J+1)\langle j_\rho j_{\rho'}; J|V|j_\rho j_{\rho'}; J\rangle}{\sum_J (2J+1)} \qquad (2)$$

is the monopole component of the neutron-proton interaction.

It is worth noting that the ESPEs coincide [26] with the energy centroids defined in [28] more than 40 years ago. The practical use of the latter definition, however, requires knowledge of all energies and spectroscopic factors corresponding to a given angular momentum, whereas expression (1) makes the computation of the ESPEs straightforward.

We have employed Eq. (1) to calculate the neutron and proton ESPEs whose values are shown in Fig. 4. By examining the various terms of Eq. (1), we see that only some of them give an important contribution to these energies. In particular, for each effective single-neutron energy in the $N = 83$ isotones, the dominant contribution is that corresponding to $\pi g_{7/2}$ due to its large occupancy. We predict, in fact, that 1.6 out of 2 protons are in the $\pi g_{7/2}$ orbit for ^{134}Te, and 3.6 out of 4 for ^{136}Xe. Note that our predicted occupancies for the ground state of ^{136}Xe are in good agreement with the results obtained from the experiment of Ref. [3]. Similar results are found for the Sb isotopes as regards the occupancy of the neutron $f_{7/2}$ orbit. The monopole matrix elements entering the dominant terms for the neutron and proton ESPEs are therefore $V^M(j_\nu \pi g_{7/2})$ and $V^M(\nu f_{7/2} j_\pi)$, respectively, which are reported in Tables VI and VII.

From Fig. 4, we see that all the neutron and proton ESPEs go down when pairs of nucleons are added. However, the decrease in energy is not the same for the various levels leading to single-particle spectra substantially different from those of the one valence-particle nuclei. For instance, the five neutron ESPEs above the lowest one tend to lie in a smaller energy interval, the $i_{13/2}$-$f_{5/2}$ spacing reducing from the initial value of 700 to 100 keV in ^{137}Xe. On the other hand, the spacing between the lowest and the highest proton levels remains practically unchanged while the three other levels move toward the $g_{7/2}$ with an overall downshift of about 500 keV in ^{137}Sb.

TABLE VI. Neutron-proton monopole components $V^M(j_\nu \pi g_{7/2})$ (in MeV).

$\nu p_{1/2}$	$\nu p_{3/2}$	$\nu f_{5/2}$	$\nu f_{7/2}$	$\nu h_{9/2}$	$\nu i_{13/2}$
−0.09	−0.11	−0.11	−0.18	−0.20	−0.33

TABLE VII. Neutron-proton monopole components $V^M(\nu f_{7/2} j_\pi)$ (in MeV).

$\pi s_{1/2}$	$\pi d_{3/2}$	$\pi d_{5/2}$	$\pi g_{7/2}$	$\pi h_{11/2}$
−0.27	−0.35	−0.28	−0.18	−0.13

In this context, it should be mentioned that the evolution of shell structure has received great attention in recent years owing to new available data on exotic nuclei, which have evidenced the appearance or disappearance of magic numbers. Several theoretical studies have then been carried out to try to identify the mechanism behind the variation of single-particle energies. In particular, the role of the monopole components of the spin-isospin and tensor interaction has been pointed out, the latter producing an attractive/repulsive effect for two unlike nucleons with opposite/aligned spin orientation [29,30]. By using the spin-tensor decomposition of the interaction, the interplay between the tensor force and other components of the neutron-proton interaction has been investigated [31]. This has provided evidence for the importance of both the central and tensor force in determining the evolution of ESPEs, the latter playing a dominant role for the energy difference of spin-orbit partners.

It would be clearly desirable to perform such a decomposition also in the present study to clarify how the behavior of the ESPEs shown in Fig. 4 is related to the various terms of our effective interaction. This is, unfortunately, not feasible since our shell-model space, on which the interaction is defined, does not contain for each orbital angular momentum the two spin-orbit partners. This is, in fact, a prerequisite to perform the spin-tensor decomposition. We cannot therefore disentangle the effects of the central and tensor force, so as to unambiguously assess the role of the various terms of the effective neutron-proton interaction in determining the evolution of the ESPEs.

From Tables VI and VII, however, we see that for each pair of neutron/proton spin-orbit partners the monopole matrix element corresponding to the orbit with opposite spin orientation relative to proton $g_{7/2}$/neutron $f_{7/2}$ is the most attractive. This accounts for the variation in the $f_{5/2}$-$f_{7/2}$ and $p_{1/2}$-$p_{3/2}$ neutron spacings, as well as in the $d_{3/2}$-$d_{5/2}$ proton one, and may be traced to the effect of the tensor component of our effective interaction [30,31]. We also predict a significant decrease in the neutron $i_{13/2}$-$h_{9/2}$ spacing, which comes essentially from $V^M(\nu i_{13/2}\pi g_{7/2})$ being more attractive than $V^M(\nu h_{9/2}\pi g_{7/2})$. The less attraction of the latter may be again attributed to the tensor force, the neutron $h_{9/2}$ orbit, unlike the $i_{13/2}$ one, being spin-down as the proton $g_{7/2}$ orbit [30]. In this connection, it is worth mentioning that this force has been shown to be responsible of the reduction in the separation of these two orbits in the $N = 83$ isotones [6,30].

V. CONCLUDING REMARKS

In this work, we have performed shell-model calculations for the four neutron-rich nuclei ^{135}Sb, ^{137}Sb, ^{135}Te, and ^{137}Xe. The main aim of our study was to follow the evolution of the single-proton and -neutron states outside doubly magic ^{132}Sn when adding neutron and proton pairs, respectively. It is worth emphasizing that in our calculations we have consistently employed the same Hamiltonian which has given a very good description of other nuclei beyond ^{132}Sn [8–10] without use of any adjustable parameters.

We have calculated energies, spectroscopic factors and effective single-particle energies for states of all the four nuclei considered and compared our results with the available experimental data which are, however, rather scanty. In particular, no spectroscopic factors are available for ^{135}Te and ^{135}Sb while no spectroscopic information at all exists for ^{137}Sb. This amounts to say that this study is largely predictive in nature and is meant to stimulate, and be of guide to, experimental efforts with RIBs in the beyond ^{132}Sn region.

Of noteworthy interest is the stronger fragmentation of the single-particle strengths predicted for ^{135}Sb and ^{137}Sb as compared to that for ^{135}Te and ^{137}Xe. This stems essentially from the fact that the neutron pairing beyond $N = 82$ is significantly smaller than the proton pairing beyond $Z = 50$. We have shown in [25] that this difference in the proton and neutron effective interaction finds its origin in core-polarization effects.

As shown in Tables II, III, and IV, our results are in very good agreement with the measured excitation energies in ^{135}Te, ^{135}Sb, and ^{137}Xe as well as with the spectroscopic factors extracted from the data for the latter. This makes us confident in the predictive power of our calculations.

ACKNOWLEDGMENT

This work has been supported in part by the Italian Ministero dell'Istruzione e della Ricerca (MIUR) under PRIN 2009.

[1] See, for instance, B. L. Cohen and R. E. Price, Phys. Rev. **121**, 1441 (1961).
[2] E. J. Schneid, A. Prakash, and B. L. Cohen, Phys. Rev. **156**, 1316 (1967).
[3] B. H. Wildenthal, E. Newman, and R. L. Auble, Phys. Rev. C **3**, 1199 (1971).
[4] K. L. Jones *et al.*, Nature (London) **465**, 454 (2010).
[5] K. L. Jones *et al.*, Phys. Rev. C **84**, 034601 (2011).
[6] B. P. Kay *et al.*, Phys. Rev. C **84**, 024325 (2011).
[7] L. Coraggio, A. Covello, A. Gargano, and N. Itaco, Phys. Rev. C **87**, 021301(R) (2013).
[8] L. Coraggio, A. Covello, A. Gargano, and N. Itaco, Phys. Rev. C **80**, 021305(R) (2009), and references therein.
[9] A. Covello, L. Coraggio, A. Gargano, and N. Itaco, Acta Phys. Pol. B **40**, 401 (2009), and references therein.
[10] A. Covello, L. Coraggio, A. Gargano, and N. Itaco, J. Phys.: Conf. Ser. **267**, 012019 (2011), and references therein.
[11] L. Coraggio, A. Covello, A. Gargano, N. Itaco, and T. T. S. Kuo, Prog. Part. Nucl. Phys. **62**, 135 (2009), and references therein.
[12] L. Coraggio, A. Covello, A. Gargano, N. Itaco, and T. T. S. Kuo, Ann. Phys. (NY) **327**, 2125 (2012), and references therein.

[13] R. Machleidt, Phys. Rev. C **63**, 024001 (2001).
[14] S. Bogner, T. T. S. Kuo, L. Coraggio, A. Covello, and N. Itaco, Phys. Rev. C **65**, 051301(R) (2002).
[15] Data extracted using the NNDC On-line Data Service from the ENSDF database version of November 20, 2012.
[16] F. Andreozzi, L. Coraggio, A. Covello, A. Gargano, T. T. S. Kuo, and A. Porrino, Phys. Rev. C **56**, R16 (1997).
[17] M. Sanchez-Vega, B. Fogelberg, H. Mach, R. B. E. Taylor, A. Lindroth, J. Blomqvist, A. Covello, and A. Gargano, Phys. Rev. C **60**, 024303 (1999).
[18] P. Hoff *et al*., Phys. Rev. Lett. **77**, 1020 (1996).
[19] W. Urban *et al*., Eur. Phys. J. A **5**, 239 (1999).
[20] B. A. Brown, A. Etchegoyen, and W. D. M. Rae, the computer code OXBASH, MSU-NSCL, Report No. 524.
[21] J. A. Cizewski *et al*., AIP Conf. Proc. **1090**, 463 (2009).
[22] J. M. Allmond *et al*., Phys. Rev. C **86**, 031307(R) (2012).
[23] L. Coraggio, A. Covello, A. Gargano, and N. Itaco, Phys. Rev. C **72**, 057302 (2005).
[24] A. Korgul, H. Mach, B. A. Brown, A. Covello, A. Gargano, B. Fogelberg, W. Kurcewicz, E. Werner-Malento, R. Orlandi, and M. Sawicka, Eur. Phys. J. A **32**, 25 (2007).
[25] A. Covello, A. Gargano, and T. T. S. Kuo, in *Fifty Years of Nuclear BCS: Pairing in Finite Systems*, edited by R. A. Broglia and V. Zelevinsky (World Scientific Publishing Company, Singapore, 2013), pp. 169–178.
[26] A. Umeya and K. Muto, Phys. Rev. C **74**, 034330 (2006).
[27] T. Duguet and G. Hagen, Phys. Rev. C **85**, 034330 (2012).
[28] M. Baranger, Nucl. Phys. A **149**, 225 (1970).
[29] T. Otsuka, R. Fujimoto, Y. Utsuno, B. A. Brown, M. Honma, and T. Mizusaki, Phys. Rev. Lett. **87**, 082502 (2001).
[30] T. Otsuka, T. Suzuki, R. Fujimoto, H. Grawe, and Y. Akaishi, Phys. Rev. Lett. **95**, 232502 (2005).
[31] N. A. Smirnova, K. Heyde, B. Bally, F. Nowacki, and K. Sieja, Phys. Rev. C **86**, 034314 (2012).